Available online at www.joac.info

ISSN: 2278-1862

Journal of Applicable Chemistry

2017, 6 (2): 241-264

(International Peer Reviewed Journal)

Corrosion Inhibition, Hydrogen Evolution and Adsorption Properties of 2-(4-Bromophenyl)-2-Oxoethyl 4-Chlorobenzoate on the Corrosion of the 18% Ni M250 Grade Maraging Steel under Weld Aged Condition in 2.0 M HCl Solution

Sanatkumar B. S[1*] and A. Nityananda Shetty[2]

1. Department of Chemistry, National Institute of Technology Karnataka, Surathkal, Srinivasnagar - 575 025, Karnataka, **INDIA**
2. Department of Basic Science and Humanities, Agnel Institute of Technology and Design, Assagao, Bardez, Goa - 403 507, **INDIA**

Email: sanatkumarbs@gmail.com

Accepted on 24th February 2017, Published online on 27th March 2017

ABSTRACT

The corrosion and corrosion inhibition of maraging steel under weld aged condition in 2.0 M HCl solution by 2-(4-Bromophenyl)-2-oxoethyl 4-chlorobenzoate (CPOM) was studied using potentiodynamic polarization technique and electrochemical impedance spectroscopy. Polarization results showed that corrosion current density, i_{corr}, and hydrogen evolution reaction decreases with increasing concentration of inhibitor in 2.0 M HCl solutions, indicating a decrease in the corrosion rate. Electrochemical impedance spectroscopy (EIS) measurements also confirmed this behaviour. Using the potentiodynamic polarization technique, the inhibitor was proved to have a mixed-type inhibition character for weld aged maraging steel by suppressing both anodic and cathodic reactions on the metal surface. The inhibition efficiency was found to increase with increase in CPOM concentration but decreased with the temperature, which is suggestive of physical adsorption mechanism. Both activation and thermodynamic parameters were calculated and discussed. The adsorption of CPOM on weld aged maraging steel surface obeys the Langmuir adsorption isotherm equation. Surface morphological studies of the weld aged maraging steel electrode surface were undertaken by scanning electron microscope (SEM) and energy dispersive X-ray spectroscopy (EDS).

Graphical Abstract: The inhibitor 2-(4-bromophenyl)-2-oxoethyl 4-chlorobenzoate (CPOM) forms thin film on the metal surface by adsorbing. This thin layer of film acts as a barrier between the acid medium and the metal surface to prevent metal from corrosion. Schematic view on behaviour of corrosion inhibitor shown in below figure.

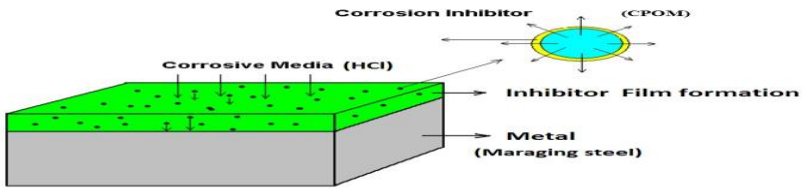

Keywords: Maraging steel, CPOM, Corrosion rate, EIS, SEM, EDS.

INTRODUCTION

The 18% Ni maraging steel is a member of the iron - nickel based alloy family. Since the steel has a very low carbon content (<0.03 wt.%), it is capable of generating a soft and ductile lath martensitic microstructure after solution treatment [1]. The development and production of maraging steel started in the early 1960s. The alloy is a low carbon steel that classically contains about 18 wt % Ni, substantial amounts of Co and Mo, together with small additions of Ti. However, depending on the demands dedicated by the application, the composition of the material can be modified. Their main strength contribution rises from the precipitation of fine and densely distributed intermetallic precipitates in a martensitic matrix. The size and type of the intermetallic precipitates depends on both the alloy composition and the applied aging treatment [2]. The high strength of maraging steel is achieved by aging at 400 - 500 ℃, where precipitation of intermetallics takes place [3]. Different grades of maraging steel are commercially available covering a strength range of 1400 - 2400 MPa [4]. Maraging steels exhibit unique combinations of ultra-high strength and excellent fracture toughness, and are taken as important material candidates for critical applications such as rocket engine cases, submarine hulls and cryogenic missiles. The automobile manufacturers and corresponding component suppliers of all over the world have been looking for ultra-high-strength materials for weight reduction or other reasons, in which maraging steel with super-high strength can be considered as a new choice [5]. Maraging steels are indispensable structural materials for high-performance military and aerospace applications [6]. Maraging steels are also used in preparation of surgical components, nuclear and gas turbines applications [7]. Thus it is a well - known fact that they frequently come into contact with acids during cleaning, pickling, decaling, acidizing, etc.

The corrosion of maraging steel is a fundamental academic and industrial concern that has received a considerable amount of attention. Using inhibitors is an important method of protecting materials against deterioration due to corrosion, especially in acidic media. The search in the literature reveals only a few reports on the corrosion studies of 18 Ni 250 grade maraging steel. Krick et al. reported that when 18 Ni maraging steel exposed to open atmosphere, undergoes more or less uniform corrosion and gets completely covered with rust [7-8]. The effect of carbonate ions in slightly alkaline medium on the corrosion of maraging steel was studied by Bellanger [9]. Bellanger and Rameau have studied the effect of slightly acidic pH with or without chloride ions in radioactive water on the corrosion of maraging steel and have reported that corrosion behaviour of maraging steel at the corrosion potential depends on pH, and intermediates remaining on the maraging steel surface in the active region favoring the passivity [10]. Maraging steels were found to be less susceptible to hydrogen embrittlement than the common high strength steels owing to the significantly low diffusion of hydrogen in them [11]. Poornima et al. have studied the corrosion behaviour of 18 Ni 250 grade maraging steel in phosphoric acid medium and reported that corrosion rate of the annealed sample is less than that of the aged sample [12]. Similar observations also have been reported for the corrosion of 18 Ni 250 grade maraging steel in sulphuric acid medium also [7]. The inhibition of corrosion for maraging steel in acid solution by organic inhibitors has been studied in considerable detail [13-14]. We have earlier reported the use of 1(2E)-1- (4 - aminophenyl)-3-(2-thienyl) prop-2-en-1- one (ATPI) as an effective inhibitor for weld aged maraging steel in 1.5 M hydrochloric acid medium [15].

A series of reports provide considerable evidence that many organic compounds could function as effective corrosion inhibitors [16-18]. The requirement for effective inhibition of hydrogen uptake is to inhibit the hydrogen evolution, to promote the hydrogen gas recombination and to inhibit the hydrogen entry. Since hydrogen evolves in corrosion processes, the inhibition of corrosion should have inhibited also

the hydrogen evolution [19]. Evolved hydrogen may recombine and leave the surface as a gas or may enter the metal causing the hydrogen - induced degradation of the metal. In order to reduce the susceptibility to hydrogen uptake, the modification of solution by addition of inhibitors or the modification of the metal surface may be applied [20]. The electronic structures of the compounds, with extensive conjugation and presence of polar N, S or O atoms, play very important roles in this regard, facilitating their adsorption on the corroding metal surfaces according to some known adsorption isotherms [21-22]. The present investigation was undertaken to elucidate the inhibiting effect of 2 - (4-Chlorophenyl)-2-oxoethyl 2-methoxybenzoate (CPOM) on the corrosion of maraging steel under weld - aged conditions in 2.0 M HCl medium at different temperatures using potentiodynamic polarization method and AC impedance (EIS) technique.

MATERIALS AND METHODS

Materials: Tests were performed on 18% Ni M250 grade maraging steel under weld aged condition. The composition of the 18% Ni M250 grade maraging steel is given in table 1. The maraging steel plates of composition as mentioned above were welded by GTAW - DCSP (Gas tungsten arc welding - Direct-current straight polarity) using filler material of compositions (wt%): 0.015% C, 17% Ni, 2.55% Mo, 12% Co, 0.015% Ti, 0.4% Al, 0.1% Mn, 0.1% Si, and the balance is Fe. The specimen was taken from the plates which are welded as per above and aged at 480 ± 5 ℃ for three hours followed by air cooling. Test coupons in the cylindrical form were cut from the plate and sealed with epoxy resin in such a way that the area exposed to the medium was 0.64 cm^2. These coupons were polished mechanically using SiC abrasive papers up to 2000 grits, finally on polishing wheel using legated alumina to obtain mirror finish. Then it was washed thoroughly with double distilled water and degreased with acetone before being immersed in the acid solution.

Table 1. Composition of the specimen (% by weight)

Element	Composition	Element	Composition
C	0.015%	Ti	0.3-0.6%
Ni	17-19%	Al	0.005-0.15%
Mo	4.6-5.2%	Mn	0.1%
Co	7-8.5%	P	0.01%
Si	0.1%	S	0.01%
O	30 ppm	N	30 ppm
H	2.0 ppm	Fe	Balance

Medium: Standard solution of 2.0 M hydrochloric acid was prepared by diluting AR grade hydrochloric acid with double distilled water. Inhibitive action of CPOM on the corrosion of weld aged maraging steel in 2.0 M HCl solution was studied by introducing different concentrations of the inhibitor into the solution. The experiments were carried out at temperatures 30 ℃, 35 ℃, 40 ℃, 45 ℃ and 50℃ (±0.5 ℃), in a calibrated thermostat. The concentration range of CPOM prepared and used in this study was 0.2 mM – 1.0 mM.

Synthesis of 2-(4-bromophenyl)-2-oxoethyl 4-chlorobenzoate (CPOM): The inhibitor 2-(4-bromo phenyl)-2-oxoethyl 4-chlorobenzoate (CPOM) was synthesized as per the reported procedure. A mixture of 4-chlorobenzoic acid (1.0 g, 0.0063mol), sodium carbonate (0.744 g, 0.0070mol) and 2-bromo-1-phenylethanonn (1.94 g, 0.0070mol) in dimethylformamide (10 mL) was stirred at room temperature for 2 h. On cooling, colourless needle-shaped crystals of 2-(4-bromophenyl)-2-oxoethyl 4-chlorobenzoate separated. The product was collected by filtration. The product was purified by recrystalization from ethanol and was identified by melting point (127 – 128 ℃), elemental analysis and infrared spectra. The molecular weight of the compound is 353.59. [23 -24] The synthesis scheme is given below.

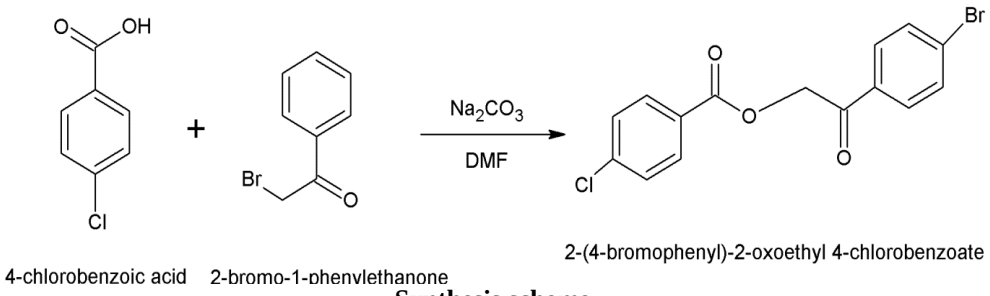

4-chlorobenzoic acid 2-bromo-1-phenylethanone 2-(4-bromophenyl)-2-oxoethyl 4-chlorobenzoate

Synthesis scheme

Electrochemical techniques: Electrochemical measurements were carried out by using an electrochemical work station, Gill AC having ACM instrument Version 5 software. The electrochemical experiments were performed in a classical three-electrode Pyrex glass cell assembly with weld aged maraging steel as the working electrode, platinum counter electrode as the auxiliary electrode, and a saturated calomel electrode (SCE) as reference. All the potentials reported are with reference to SCE. Before measurement, the working electrode was immersed in test solution for approximately 15 min until a steady open-circuit potential (OCP) was reached. The polarization studies were done immediately after the EIS studies on the same electrode without any further surface treatment.

Potentiodynamic polarization studies: Finely polished weld aged maraging steel specimen was exposed to the corrosion medium of 2.0 M hydrochloric acid in the presence and absence of the inhibitor at different temperatures (30 - 50 ℃) and allowed to establish a steady - state open circuit potential (OCP). The potentiodynamic current - potential curves were recorded by polarizing the specimen to -250 mV cathodically and +250 mV anodically with respect to the OCP at a scan rate of 1 mV s^{-1}.

Electrochemical impedance spectroscopy studies (EIS): The corrosion behaviour of the weld aged maraging also obtained from EIS technique by using electrochemical work station. The impedance measurements were carried out in the frequency range of 10 KHz to 0.01 Hz, at the rest potential, by applying 10 mV sine wave AC voltage. The double layer capacitance (C_{dl}), the charge transfer resistance (R_{ct}), film capacitance (C_f) and film resistance (R_f) were calculated from the Nyquist plot. Several runs were performed for each measurement to obtain reproducible data.

Scanning Electron Microscopic (SEM) and EDS analysis: The scanning electron microscopic images and EDS spectra of the samples were recorded using JEOL JSM–6380L Analytical scanning electron microscope.

RESULTS AND DISCUSSION

Potentiodynamic polarization measurement: Potentiodynamic polarization curves of weld aged maraging steel in 2.0 M HCl solution without and with different concentrations of CPOM are shown in figure 1, at 30 ℃. Similar plots were obtained at other temperatures also. Corrosion parameters, such as corrosion potential (E_{corr}), corrosion current density (i_{corr}), cathodic and anodic Tafel slopes (β_c and β_a), and the inhibition efficiency η (%) associated with the polarization measurements for the alloy at different temperatures in the presence of different concentrations of CPOM are summarized in table 2. It is usually assumed that the process of oxidation is uniform and does not occur selectively to any component of the alloy. Equivalent weight (EW) for alloys was calculated from following equation:

$$EW = \frac{1}{\Sigma \frac{n_i f_i}{W_i}} \qquad (1)$$

Where f_i is the mass fraction of the i^{th} element in the alloy, W_i is the atomic weight of the i^{th} element in the alloy and n_i is the valence of the i^{th} element of the alloy [25].
The inhibition efficiency was calculated from following equation:

$$\eta(\%) = \frac{i_{corr} - i_{corr(inh)}}{i_{corr}} \times 100 \qquad (2)$$

where i_{corr} and $i_{corr(inh)}$ signify the corrosion current density in the absence and presence of inhibitors, respectively.[26]
The corrosion rate (υ_{corr}), in mmy^{-1}, is calculated from following equation:

$$Corrosion\ rate\ (\upsilon_{corr}) = K\frac{i_{corr}}{\rho}EW \qquad (3)$$

where K is 3.27×10^{-3}, mm g/μA cm yr, a constant that defines the unit for the corrosion rate, i_{corr} is current density in A cm^{-2}, ρ density is in g cm^{-3} and EW is equivalent weight of the alloy [25].

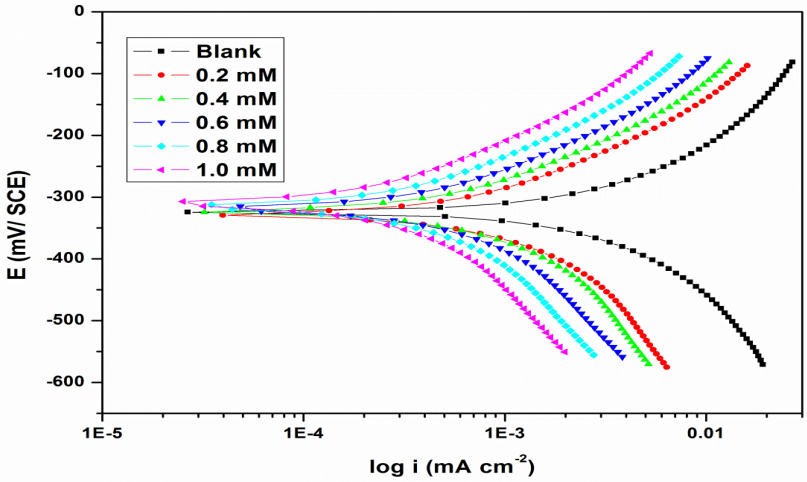

Fig. 1 Tafel polarization curves for the corrosion of weld aged maraging steel in 2.0 M HCl containing different concentrations of inhibitor at 30 ℃.

A closer look at the polarisation curves shows that the addition of CPOM decreases the corrosion of the weld aged maraging steel sample. It could be observed that both the cathodic and anodic reactions were suppressed with the addition of CPOM, which suggested that the inhibitor exerted an efficient inhibitory effect both on anodic dissolution of metal and on cathodic hydrogen reduction reaction [27]. According to available literature, hydrogen evolution reaction has been reported to be generally the dominant local cathodic process in the corrosion of steel alloy in aqueous acidic solutions, via H^+ ion or H_2O molecule reduction, respectively. The amounts of hydrogen evolved by the cathodic reaction are proportional to the corroded amounts of iron. The increase of the corrosion rate and rate of hydrogen evolution can be rationalized on the basis that acid reacts with iron and forms metal salts (metal chloride), which are soluble in aqueous media [20]. In cathodic domain, as seen in table 2, the values of β_c had small changes with increasing inhibitor concentration, which indicated that the CPOM was adsorbed on the metal surface and the addition of the inhibitor hindered the acid attack on the maraging steel electrode [27]. The parallel cathodic Tafel curves showed that the hydrogen evolution was activation controlled and the reduction mechanism was not affected by the presence of the inhibitor [28]. In anodic domain, the value of β_a

decreases with the presence of CPOM. The shift in the anodic Tafel slope β_a might be attributed to the modification of anodic dissolution process due to the inhibitor modules adsorption on the active sites [27]. This indicates that the inhibitive action of CPOM may be considered due to the adsorption and formation of barrier film on the electrode surface. The barrier film formed on the metal surface reduces the probability of both the anodic and cathodic reactions. Thus, the inhibitor, CPOM can be considered as a mixed type of inhibitor [14]. The data in the table 2 clearly show that the CPOM effectively decreases the corrosion current density (i_{corr}) of the weld aged maraging steel, even when added in small concentrations.

Table 2. Results of potentiodynamic polarization studies on weld aged maraging steel in 2.0 M HCl containing different concentrations of CPOM

Temperature (℃)	Conc. of inhibitor (mM)	E_{corr} (mV /SCE)	b_a (mV dec^{-1})	$-b_c$ (mV dec^{-1})	i_{corr} (mA cm^{-2})	υ_{corr} (mm y^{-1})	η (%)
30	Blank	-324	175	287	3.08	35.4	
	0.2	-327	173	291	1.65	19.0	46.4
	0.4	-322	168	285	1.24	14.2	59.6
	0.6	-318	170	282	0.92	10.5	70.0
	0.8	-315	165	278	0.57	6.5	81.2
	1.0	-310	159	274	0.33	3.8	89.0
35	Blank	-325	189	307	3.50	40.3	
	0.2	-323	193	305	1.94	22.3	44.6
	0.4	-319	186	303	1.52	17.5	56.5
	0.6	-320	183	299	1.11	12.7	68.1
	0.8	-316	178	295	0.74	8.5	78.6
	1.0	-313	175	293	0.45	5.1	86.9
40	Blank	-321	192	325	3.88	44.7	
	0.2	-324	188	322	2.22	25.5	42.8
	0.4	-320	185	317	1.78	20.5	54.1
	0.6	-318	181	319	1.32	15.2	65.8
	0.8	-315	176	312	1.03	11.8	75.6
	1.0	-310	170	309	0.60	6.9	84.3
45	Blank	-322	206	332	4.18	48.1	
	0.2	-318	208	330	2.49	28.6	40.2
	0.4	-320	203	335	2.02	23.2	51.6
	0.6	-317	198	327	1.59	18.3	61.9
	0.8	-314	195	323	1.13	13.0	72.8
	1.0	-309	191	319	0.82	9.4	80.2
50	Blank	-319	224	340	4.51	51.9	
	0.2	-322	227	337	2.76	31.7	38.6
	0.4	-324	221	332	2.30	26.4	48.7
	0.6	-321	218	335	1.88	21.6	58.2
	0.8	-315	214	330	1.47	16.9	67.3
	1.0	-307	211	326	1.05	12.0	76.7

The presence of inhibitor brings down the corrosion rate considerably. Polarization curves are shifted to a lower current density region indicating a decrease in corrosion rate (υ_{corr}) [29]. Inhibition efficiency increases with the increase in the inhibitor concentration up to an optimum value. There after the increase in the inhibitor concentration resulted in negligible increase in inhibition efficiency. The maximum quantity of the inhibitor reported in table 2 corresponds to the optimum concentration of the inhibitor. The

highest η (%) may be attributed to its adsorption on the metal surface through polar groups (OCH_2, CO or O) as well as through π - electrons of the double bond [30]. This also can be attributed to deposition of the inhibitor molecules by increasing concentration on the alloy as a result of interaction between the inhibitor and the metal surface especially Cr, Ni and Mo that can form oxides which effectively seals the surface against further reaction [19].

Corrosion potential (E_{corr}) values shift towards little positive potential as the inhibitor concentration increases, indicating passivation of iron through adsorption of CPOM reflecting the formation of protective films on the electrode surface. This may be due to the blocking of the surface by both adsorption and film formation mechanism [30]. On studying the effect of concentration for this compound from 0.2 mM to1.0 mM, it is noticed that the presence of inhibitor does not cause any significance shift in the E_{corr} value. According to Riggs and others, if the displacement in corrosion potential is more than ±85 mV with respect to the corrosion potential of the blank, the inhibitor can be considered a distinctive cathodic or anodic type [31]. However, the maximum displacement in this study is ±16 mV. This implies that the inhibitor, CPOM, acts as a mixed type inhibitor, affecting both anodic and cathodic reactions [13].

Electrochemical impedance spectroscopy studies (EIS): The corrosion behaviour of weld aged maraging steel in 2.0 M HCl solution in the presence and absence of CPOM was investigated by electrochemical impedance spectroscopy. Figure 2 shows the Nyquist plots for the corrosion of weld aged maraging steel in 2.0 M HCl solution at 30 ºC in the presence of different concentrations of CPOM. Similar plots were obtained at other temperatures also. The Nyquist plots for the blank (without inhibitor) tests at different temperatures are used as reference for results with inhibitor at various concentrations. From figure 2, it can be observed that the impedance spectra show a single semicircle and the diameter of semicircle increases with increasing inhibitor concentration. The semicircle in all cases corresponds to a capacitive loop and the semicircle radii depend on the inhibitor concentration [26]. These diagrams exhibit that the impedance spectra consist of single capacitive loop at high frequency, the high frequency capacitive loop was attributed to charge transfer of the corrosion process. The increase in diameter of the semicircle with the increase in the CPOM concentration, indicating the increase in charge transfer resistance (R_{ct}) value and decrease in corrosion rate (υ_{corr}) [32]. Then, it is noticed that the impedance spectra did not present perfect semicircles. The ‘‘depressed’’ semicircles have a centre under the real axis, and can be seen as depressed capacitive loops. Such phenomena often correspond to surface heterogeneity which may be the result of surface roughness, dislocations, distribution of the active sites or adsorption of inhibitor [14]. The presence of inhibitor increases the impedance but does not change other aspects of the behaviour. These results support the results of polarization measurements that the inhibitor does not alter the mechanism of electrochemical reactions responsible for corrosion [15].

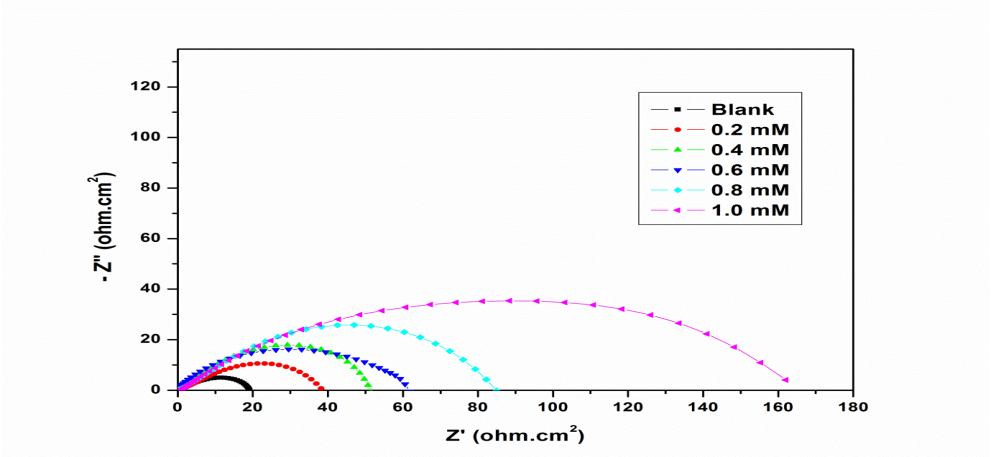

Fig. 2 Nyquist plots for the corrosion of weld aged maraging steel specimen in 2.0 M HCl containing different concentrations of inhibitor at 30 ℃.

In order to fit and analyze the EIS data, the experimental impedance results are simulated to pure electronic models that can verify or role out mechanistic models and enable the calculation of numerical values corresponding to the physical and/or chemical properties of the electrochemical system under investigation. The equivalent circuits were selected and are shown in figure 3. These circuits are generally used to describe the iron/acid interface model [33]. The circuit fitment was done by ZSimpWin software version 3.21. The standard Randles' circuit model was used for the blank solution (without inhibitor), and is shown in Figure 3a. This circuit shows good simulations for the experimental data. The equivalent circuit consists of a parallel combination of charge-transfer resistance (R_{ct}) and constant phase element (*CPE, Q*), both in series with the solution resistance (R_s). A constant-phase element (*CPE*) is employed instead of the double layer capacitance (C_{dl}) to describe the non-homogeneities in the system. R_{ct} is a resistance to the corrosion process. That resistance can be present as the charge-transfer resistance at the metal/oxide film interface, the resistance of the oxide film, and/or the charge transfer resistance at the oxide film/solution interface [26]. The *CPE* impedance (Z_{CPE}) is given by the expression:

$$Z_{CPE} = \frac{1}{Q} \times \frac{1}{(j\omega)^n} \qquad (4)$$

where *Q* is the *CPE* coefficient, *n* is the *CPE* exponent (phase shift), ω is the angular frequency ($\omega = 2\pi f$, where *f* is the AC frequency) and *j* is the imaginary unit. When the value of *n* is 1, the *CPE* behaves like an ideal double-layer capacitance (C_{dl}). The correction of capacity to its real values is calculated from the expression: [26].

$$C_{dl} = Q(\omega_{max})^{n-1} \qquad (5)$$

where ω_{max} is the frequency at which the imaginary part of impedance ($-Z_i$) has a maximum [34] . The data obtained from fitted spectra are listed in table 3.The physical meaning of a *CPE* has been discussed by many authors and can represent all frequency - dependant electrochemical phenomena, namely double-layer capacitance (α =1) and diffusion processes (α = 0.5) as well as local frequency dispersion due to surface heterogeneity. Q_{dl} is introduced instead of C_{dl} in time constant which belongs to corrosion process and represents an experimental deviation from the semi-circle. According some literature report the time constants which represent corrosion process are not given as semi-circle but given as semi-ellipse and they also suggest new equivalent circuit model [35]. The Nyquist plots obtained in the real system represent a general behaviour where the double layer on the interface of metal/solution does not behave as a real capacitor. On the metal side electrons control the charge distribution whereas on the solution side it is controlled by ions. As ions are much larger than the electrons, the equivalent ions to the charge on the metal will occupy quite a large volume on the solution side of the double layer [26].

For an approximate description of the EIS measurements in inhibited solution, an equivalent circuit is suggested, and is shown in Figure 3(b). Excellent fit with this model was obtained for all concentrations and temperatures. Here, CPE_1 element is considered as a model of double layer capacitance (C_{dl}) like H_2O and other ion adsorbed on the surface of metal sample, and CPE_2 as a model of film capacitance (C_f), R_{ct} is the charge transfer resistance and R_f is film resistance. The representative fitting results are given in table 3. The fitting results (see Table 3) show that C_{dl} and C_f (film capacitance) decrease, R_{ct} and R_f (film resistance) increase with increasing concentration of CPOB, suggesting that the amount of the inhibitor molecules adsorbed on the electrode surface increases. This decrease in C_{dl} and C_f could be attributed to the decrease in local dielectric constant and/or an increase in the thickness of the electrical double layer, signifying that the CPOB molecule acts by adsorption at the interface of metal/solution [36]. In addition, the more the inhibitor is adsorbed, the more the thickness of the barrier layer is increased according to the expression of the Helmholtz model: [27]

$$C_{dl} = \frac{\varepsilon^o \varepsilon}{d} S \qquad (6)$$

Where d is the thickness of the film, S the surface of the electrode, ε^o the permittivity of the air and ε is the local dielectric constant.

The change in R_{ct}, R_f, C_{dl} and C_f values was caused by the gradual replacement of water molecules by adsorption of the inhibitor molecules on the metal surface, reducing the extent of acidic dissolution for the weld aged maraging steel [36].

The related inhibitor efficiency η (%) was calculated by the charge transfer resistance as follows:

$$\eta(\%) = \frac{R_{ct(inh)} - R_{ct}}{R_{ct(inh)}} \times 100 \qquad (7)$$

where $R_{ct(inh)}$ and R_{ct} are the charge transfer resistances obtained in inhibited and uninhibited solutions, respectively [13].

The corrosion current density i_{corr} can be calculated using the charge transfer resistance value, R_{ct}, using with the Stern–Geary equation [37].

$$i_{corr} = \frac{b_a b_c}{2.303(b_a + b_c) R_{ct}} \qquad (8)$$

Inhibition efficiency η (%) increases with increasing inhibitor concentration. This is attributed to increasing inhibitor concentration that leads to an increase in surface coverage. This layer makes a barrier for mass and charge transfer for metal dissolution [32]. Thus, it was found that CPOM has the highest total resistance value due to it has the most electron rich environment in phenyl group due to resonance of π electrons of double bonds that can be adsorbed well on the sample surface [18]. Also methoxy and carbonyl group is electron donating group containing oxygen atom as an active group [20]. Such action could be explained through the lone pair of non-bonding electrons one - OCH_3 group which is freely to liberate its lone pair into the system than methyl group [19]. It is considered that the rate of adsorption is usually rapid and hence, the reactive metal surface is shielded from the aggressive acid environment and thus decreasing hydrogen evolution on the electrode surface. The obtained Bode plot for CPOM is shown in figure 4. Bode plots are recommended as standard impedance plots, since all experimental impedance data are equally represented and the phase angle as a sensitive parameter to interfacial phenomena appears explicitly [18]. The high frequency (*HF*) limits correspond to R_s *(Ω),* while the lower frequency (*LF*) limits corresponds to (R_{ct} + R_s), which is associated with the dissolution processes at the interface. The low frequency contribution shows the kinetic response of the charge transfer reaction [32]. Phase angle increases with increase in concentrations of CPOM in hydrochloric acid medium. The difference between the *HF* and *LF* for the inhibited system in the Bode plot increases with increase in the concentration of CPOB. This might be due to decrease in dissolution of metal and decrease in capacitive behaviour on the metal surface. The presence of one phase maximum at intermediate frequencies indicates the presence of one time constant corresponding to the impedance of the formed adsorbed film. The adsorption of CPOM on the metal surface modifies the interface between solution and metal surface and decreases its electrical capacity [22]. This modification results in an increase of charge transfer resistance where the resulting adsorption films isolate the metal surface from the corrosive medium and decrease metal dissolution [38-39]. At the highest inhibitor concentration of 1.0 mM, the inhibition efficiency was increased markedly

and reached 87.2 %. Furthermore, the values of inhibition efficiency obtained potentiodynamic polarization measurements and EIS measurements are in good agreement.

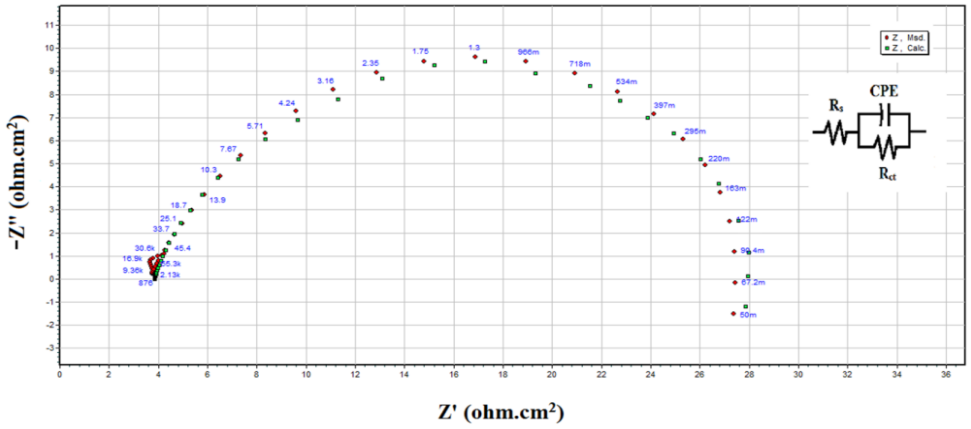

Fig. 3 (a): Equivalent circuit used to fit the experimental EIS data for the corrosion of weld aged maraging steel specimen in 2.0 M HCl acid at 30 ℃ for blank solution.

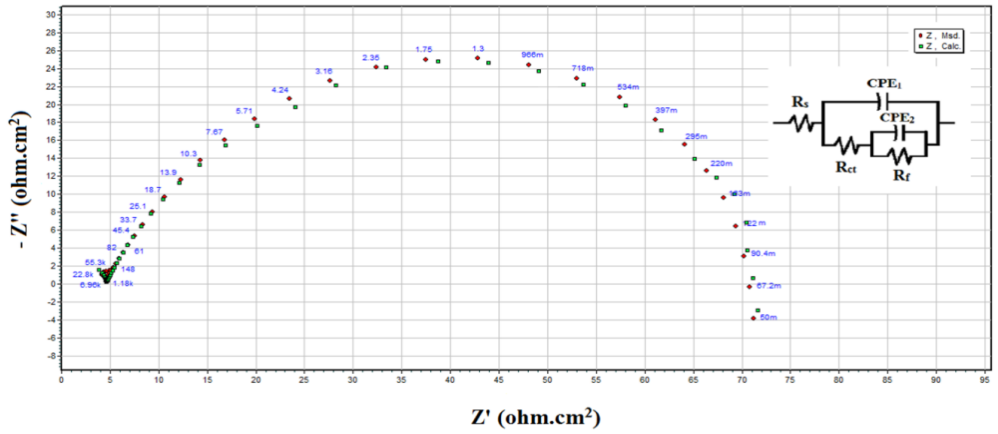

Fig.3 (b): Equivalent circuit used to fit the experimental EIS data for the corrosion of weld aged maraging steel specimen in 2.0 M HCl acid at 30 ℃ in presence of different concentration of inhibitors.

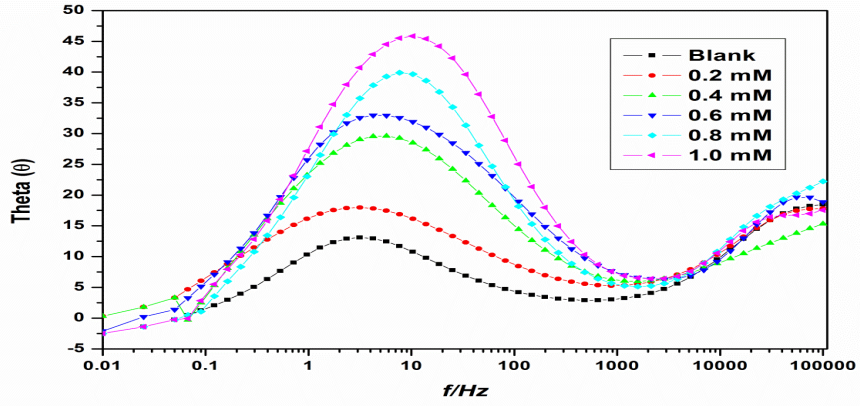

Fig. 4 Bode plots for the corrosion of weld aged maraging steel specimen in 2.0 M HCl containing different concentrations of inhibitor at 30 ℃.

Table 3. EIS data of weld aged maraging steel in 2.0 M HCl containing different concentrations of CPOM

Temperature (℃)	Conc. of inhibitor (mM)	R_{ct} (ohm. cm^2)	C_{dl} (mF cm^{-2})	R_f (ohm. cm^2)	C_f (mF cm^{-2})	η (%)
30	Blank	20	5.7	1.2		
	0.2	39	3.1	1.9	0.82	48.7
	0.4	48	2.84	2.8	0.64	58.4
	0.6	61	2.11	3.6	0.46	67.2
	0.8	87	1.56	4.9	0.33	77.0
	1.0	157	0.83	8.8	0.21	87.2
35	Blank	18.0	8.2	0.9		
	0.2	33.0	5.23	1.6	1.36	45.4
	0.4	41.0	4.79	2.5	0.89	56.0
	0.6	54.4	3.67	3.3	0.63	65.9
	0.8	74.2	2.98	4.4	0.52	75.7
	1.0	116	2.05	7.9	0.31	84.4
40	Blank	15.5	13.2	0.8		
	0.2	27.0	7.44	1.52	1.89	42.5
	0.4	33.3	5.35	2.2	1.22	53.4
	0.6	41.5	4.76	3.1	0.92	62.6
	0.8	57.4	4.11	4.0	0.78	72.9
	1.0	89.3	3.05	6.8	0.45	82.6
45	Blank	13.2	15.7	0.7		
	0.2	21.5	10.6	1.3	2.40	38.6
	0.4	26.4	7.02	1.9	1.73	50.0
	0.6	32.6	5.89	2.8	1.45	59.5
	0.8	44.8	4.35	3.7	0.92	70.5
	1.0	73.2	3.23	6.0	0.61	81.9
50	Blank	11.0	16.3	0.5		
	0.2	17.1	12.7	0.9	3.16	35.6
	0.4	20.1	9.52	1.5	2.62	46.2
	0.6	24.8	7.76	2.3	1.99	55.6
	0.8	32.4	6.10	3.1	1.35	66.0
	1.0	51.0	4.24	5.4	0.91	78.4

Effect of temperature: The study on the effect of temperature on the corrosion rate and inhibition efficiency facilitates the calculation of kinetic and thermodynamic parameters for the inhibition and the adsorption processes. These parameters are useful in interpreting the type of adsorption by the inhibitor [27]. The results in tables 4 and 5 show that corrosion rate increases and the inhibition efficiency of CPOM decreases with the increase in temperature. The decrease in inhibition efficiency with the increase in temperature indicates desorption of the inhibitor molecules from the metal surface on increasing the temperature [13]. In this study, with increase in solution temperature, corrosion potential (E_{corr}), anodic Tafel slope (b_a), and cathodic Tafel slope (b_c) values are not affected much. This indicates that increase in temperature does not change the mechanism of corrosion reaction [14]. The inhibition efficiency decreases with increase in temperature which indicates desorption of inhibitor molecules. This may be attributed to

the higher dissolution rates of weld aged maraging steel at elevated temperature and also a possible desorption of adsorbed inhibitor due to increased solution agitation resulting from higher rates of hydrogen gas evolution, which may also reduce the ability of the inhibitor to be adsorbed on the metal surface. The decrease in R_{ct} and inhibition efficiency with the increase in temperature indicates desorption of the inhibitor molecules from the metal surface on increasing the temperature. This fact is also suggestive of physisorption of the inhibitor molecules on the metal surface [40]. The activation parameters for the dissolution of weld aged maraging steel in 2.0 M HCl both in the absence and presence of various concentrations of CPOB were obtained from the Arrhenius equation: 41

$$\ln(\upsilon_{\text{corr}}) = B - \frac{E_{\text{a}}}{RT} \qquad (9)$$

where E_a is apparent activation energy for the corrosion process in the presence and absence of inhibitor, B is a constant which depends on the metal type, R is the universal gas constant and T is the absolute temperature. The plot of $ln(\upsilon_{corr})$ versus reciprocal of absolute temperature ($1/T$) gives a straight line with slope = - E_a / R, from which, the activation energy values for the corrosion process were calculated [19].

The Arrhenius plots for the corrosion of weld aged maraging steel in the presence of different concentrations of CPOM in 2.0 M HCl acid are shown in figure 5.

The entropy of activation ($\Delta H^{\#}$) and enthalpy of activation ($\Delta S^{\#}$) for the corrosion of alloy were calculated from the transition state theory Equation: [21].

$$\upsilon_{corr} = \frac{RT}{Nh}\exp\left(\frac{\Delta S^{\#}}{R}\right)\exp\left(\frac{-\Delta H^{\#}}{R}\right) \qquad (10)$$

where h is Plank's constant, and N is Avagadro's number. The plots of $ln(\upsilon_{corr}/T)$ versus $1/T$ in 2.0 M HCl acid in the absence and presence of various concentrations of CPOB is shown in Fig. 6. The calculated values of E_a, $\Delta H^{\#}$ and $\Delta S^{\#}$ are given in table 4.

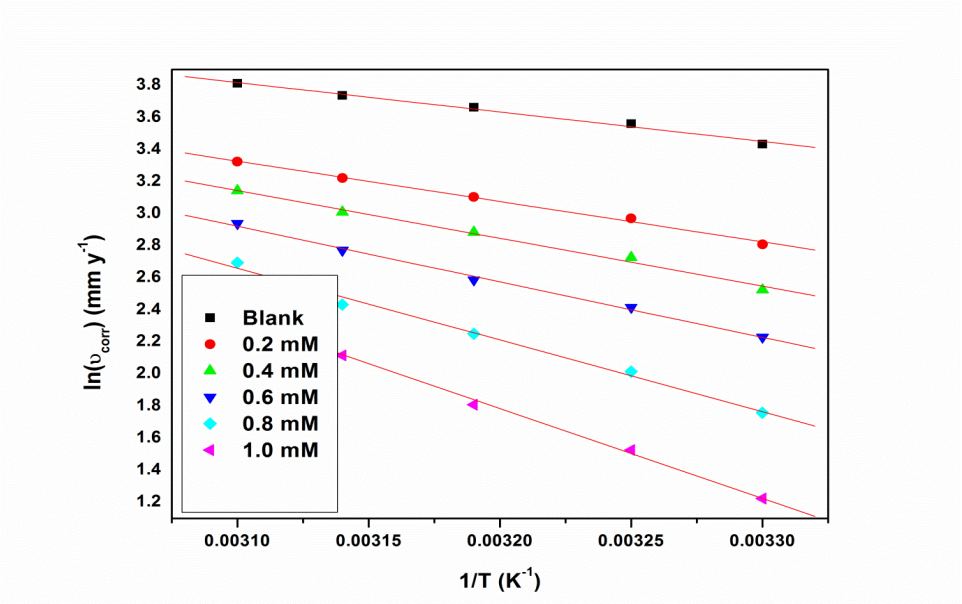

Fig. 5 Arrhenius plots for the corrosion of weld aged maraging steel in 2.0 M HCl containing different concentrations of inhibitor.

Table 4. Activation parameters for the corrosion of weld aged maraging steel in 2.0 M HCl containing different concentrations of inhibitor

Conc. of inhibitor (mM)	E_a (kJ^{-1} mol^{-1})	$\Delta H^{\#}$ (kJ^{-1} mol^{-1})	$\Delta S^{\#}$ (J mol^{-1} K^{-1})
Blank	20.25	12.65	-174.62
0.2	22.90	18.31	-161.15
0.4	24.75	22.148	-150.84
0.6	28.82	26.22	-140.00
0.8	37.18	34.59	-132.92
1.0	45.59	43.97	-97.81

Table 5. Thermodynamic parameters for the adsorption of CPOM on weld aged maraging steel surface in 2.0 M HCl at different temperatures.

Temperature (℃)	$-\Delta G^{o}_{ads}$ (kJ mol^{-1})	ΔH^{o}_{ads} (kJ mol^{-1})	ΔS^{o}_{ads} (J mol^{-1} K^{-1})
30	30.50	- 10.56	-65.8
35	30.83		
40	31.18		
45	31.48		
50	31.82		

The chemically stable surface active inhibitors increase the energy of activation and decrease the surface area available for corrosion. The data in the table 4 show that the values of E_a of the corrosion of weld aged maraging steel in the 2.0 M hydrochloric acid medium in the presence of CPOM are higher than those in the uninhibited medium. The increase in the E_a values, with increasing inhibitor concentration indicates the increase in energy barrier for the corrosion reaction, with the increasing concentrations of the inhibitor [42]. It is also indicated that the whole process is controlled by surface reaction, since the activation energies of the corrosion process are above20 kJ mol^{-1}. The adsorption of the inhibitor on the electrode surface leads to the formation of a physical barrier between the metal surface and the corrosion medium, blocking the charge transfer, and thereby reducing the metal reactivity in the electrochemical reactions of corrosion [13]. The decrease in the inhibition efficiency of CPOM with the increase in temperature can be considered to be because of the decrease in the extent of adsorption of the inhibitor on the metal surface with the increase in temperature, and corresponding increase in corrosion rate as a greater area of the metal surface is exposed to the corrosion medium. The observations also support the view that the inhibitor is adsorbed on the metal surface through physisorption. In other words, the adsorption of the inhibitor on the electrode surface leads to the formation of a physical barrier that reduces the metal reactivity in the electro chemical reactions of corrosion [14]. The entropy of activation ($\Delta S^{\#}$) values are less negative for inhibited solutions than that for the uninhibited solutions. This suggested that a decrease in randomness occurred on going from reactants to the activated complex [43]. This might be the results of the adsorption of organic inhibitor molecules from the acidic solution which could be regarded as a quasi-substitution process between the organic compound in the aqueous phase and water molecules at electrode surface [44]. The adsorption of organic inhibitor is accompanied by desorption of water molecules from the surface. Thus the increasing in entropy of activation may be attributed to the increase in solvent entropy [45].

Adsorption isotherm: In order to understand the mechanism of corrosion inhibition, the adsorption behaviour of the organic adsorbate on metal surface must be known. As far as the inhibition process is concerned, it is generally assumed that the adsorption of the inhibitors at the metal solution interface is the first step in the action mechanism of inhibitors in aggressive acid media [20]. Inhibition of corrosion of weld aged maraging steel in 2.0 M HCl solution by the CPOM can be explained on the basis of adsorption.

Four types of adsorption may take place involving organic molecules at the metal solution interface: (i) electrostatic attraction between charged molecules and the charged metal, (ii) interaction of unshared electron pairs in the molecule with the metal, (iii) interaction of π-electrons with the metal and (iv) combination of the above [30]. It is apparent that the adsorption of CPOM compound on the metal surface could occur directly on the basis of donor acceptor interaction between the lone pairs of the heteroatoms and the extensively delocalised π-electrons of the CPOM molecule and the vacant d-orbitals of iron surface atoms. Moreover, the presence of oxygen substituent in the organic structures makes the formation of dπ-dπ bond resulting from overlap of 3d electrons from Fe atom to the 3d vacant orbital of the oxygen atom possible, which enhances the adsorption of the compounds on the metal surface. These compounds inhibit the corrosion by controlling both the anodic and cathodic reactions. In acidic solution, CPOM can exist as protonated species. The protonated species may adsorb on the cathodic sites of the metal surface and decrease the evolution of hydrogen. The adsorption of these compounds on anodic sites may decrease anodic dissolution of weld aged maraging steel [13-14]. The adsorption of an organic adsorbate on a metal solution interface can be represented as a substitution process between the organic molecules in the aqueous solution ($Org_{(sol)}$) and the water molecules on the metallic surface ($H_2O_{(ads)}$) as represented below: [27].

$$Inh_{(sol)} + \chi H_2O_{(ads)} \leftrightarrow Org_{(ads)} + \chi H_2O_{(sol)} \qquad (11)$$

where $Org_{(sol)}$ and $Org_{(ads)}$ are the organic molecules in the aqueous solution and adsorbed on the metallic surface, respectively; $H_2O_{(ads)}$ and $H_2O_{(sol)}$ are the water molecules on the metallic surface and in the solution, respectively; and χ represents the number of water molecules replaced by one molecule of organic adsorbate. Thus, in aqueous acidic solution, CPOM exists partly in the form of protonated species and partly as neutral molecules [28]. Also, the adsorption provides information about the interaction among the adsorbed molecules themselves as well as their interaction with the electrode surface. Actually an adsorbed molecule may make the surface more difficult or less difficult for another molecule to become attached to a neighbouring site and multilayer adsorption may take place. There may be more or less than one inhibitor molecule per surface site. Finally, various surface sites could have varying degree of activation [46].

The data were applied to various isotherms including Langmuir, Temkin, Frumkin and Flory-Huggins isotherms. It was found that the data fitted best with the Langmuir adsorption isotherm.

$$\frac{C_{inh}}{\theta} = C_{inh} + \frac{1}{K} \qquad (12)$$

where K is the adsorption/desorption equilibrium constant, C_{inh} is the corrosion inhibitor concentration in the solution, and θ is the surface coverage, which is calculated using equation: [36]

$$\theta = \frac{\eta(\%)}{100} \qquad (13)$$

where $\eta(\%)$ is the percentage inhibition efficiency. The plots of C_{inh}/θ versus C_{inh} gives a straight line(Figure 6) with an intercept of $1/K$. The Langmuir adsorption isotherms for the adsorption of CPOM on the maraging steel surface are shown in figure 7. The plots are linear, with an average correlation coefficient of 0.9734. It is seen that the Langmuir adsorption isotherm is best applicable at 40℃ (R^2 = 0.9788).

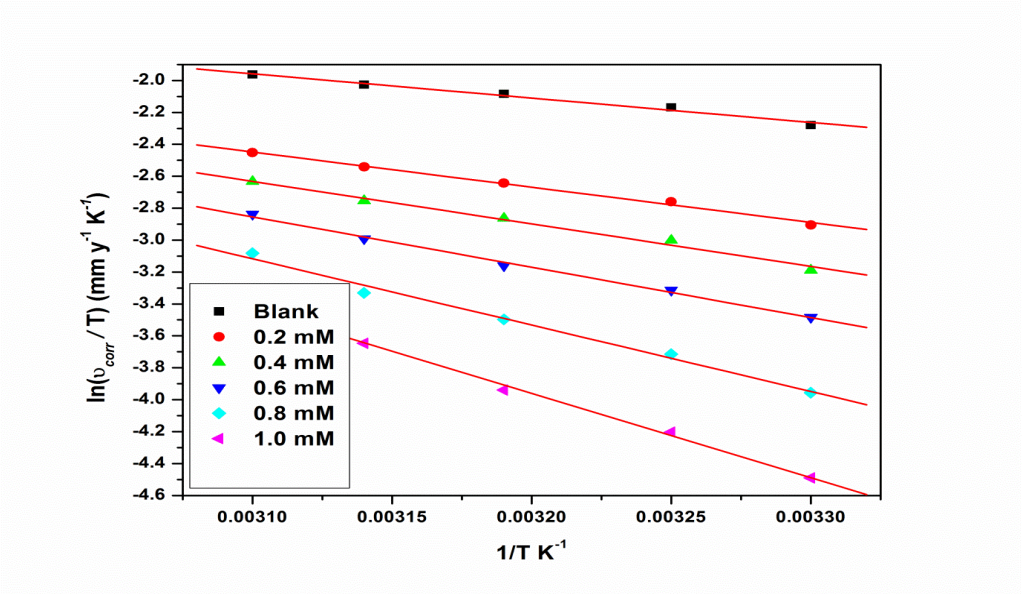

Fig. 6 Plots of $\ln(\upsilon_{corr}/T)$ versus 1/T for the corrosion of weld aged maraging steel in 2.0 M HCl containing different concentrations of inhibitor.

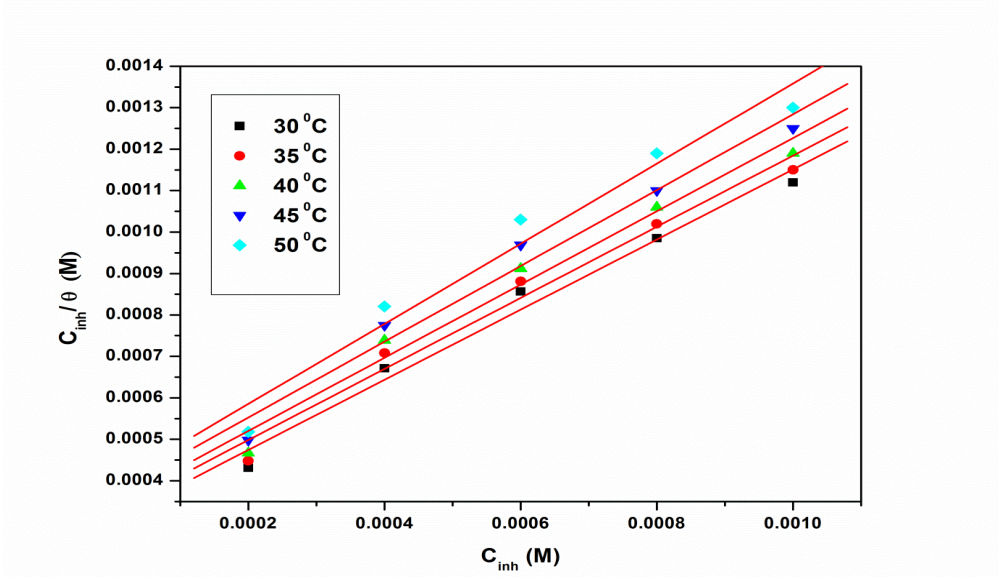

Fig. 7 Langmuir adsorption isotherms for the adsorption of ATPI on weld aged maraging steel in 2.0 M HCl at different temperatures.

The values of standard free energy ΔG^0_{ads} of adsorption are related to K by the relation: [20]

$$K = \frac{1}{55.5}\exp\left(\frac{-\Delta G^0_{ads}}{RT}\right) \qquad (14)$$

where the value 55.5 is the concentration of water in solution in mol dm^{-3}, R is the universal gas constant and T is absolute temperature. Standard enthalpy of adsorption (ΔH^0_{ads}) and standard entropies of adsorption (ΔS^0_{ads}) were obtained from the plot of (ΔG^0_{ads}) versus T according to the thermodynamic equation: [47]

$$\Delta G^0_{ads} = \Delta H^0_{ads} - T\Delta S^0_{ads} \quad (15)$$

The thermodynamic data obtained are tabulated in table 5. The plot of (ΔG^0_{ads}) / T shown in figure 8.

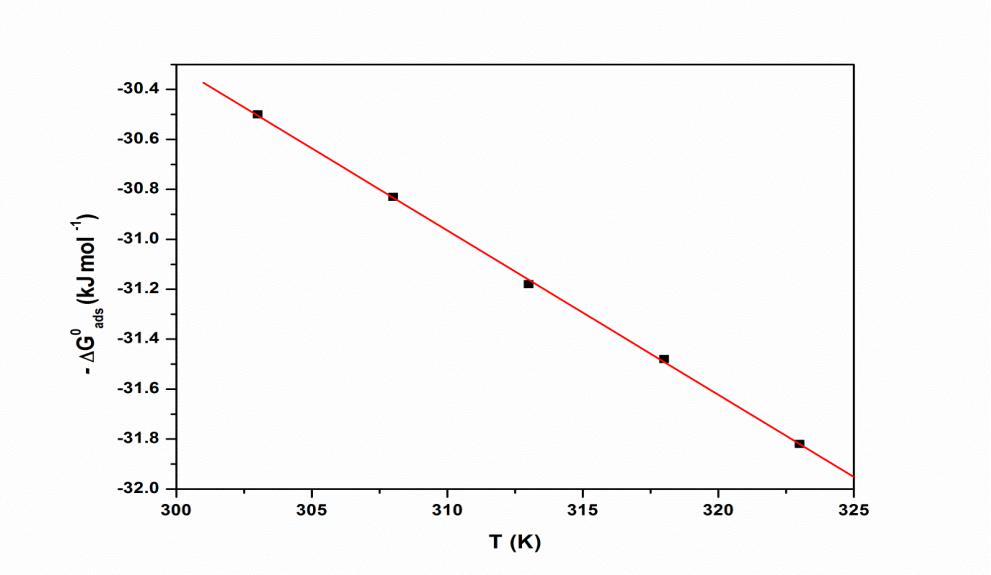

Fig. 8 The plot of (ΔG^0_{ads}) / T for the adsorption of CPOM on weld aged maraging steel in 2.0 M HCl.

In general, an endothermic adsorption process ($\Delta H^0_{ads} > 0$) is attributed unequivocally to chemisorption, an exothermic adsorption process ($\Delta H^0_{ads} < 0$) may involve either physisorption or chemisorption or a combination of both the processes. In an exothermic process, the physisorption is distinguished from the chemisorption by considering the absolute values of standard enthalpies of adsorption [14]. The negative sign of ΔH^0_{ads} in 2.0 M HCl solution indicates that the adsorption of inhibitor molecule is an exothermic process. Generally, an exothermic adsorption process signifies either physisorption or chemisorptions while endothermic process is attributable unequivocally to chemisorption. Typically, the standard enthalpy of physisorption process is less negative than 41.86 kJ mol^{-1}, while that of chemisorptions process approaches to 100 kJ mol^{-1} [30]. In the present study the value of ΔH^0_{ads} is -10.56 kJ mol^{-1}, which show that the adsorption of CPOM on weld aged maraging steel involves physisorption phenomenon.

The negative values of ΔG^0_{ads} indicate the spontaneity of the adsorption process and the stability of the adsorbed layer on the metal surface [27]. Generally the values of ΔG^0_{ads} less than -20 kJ mol^{-1} are consistent with physisorption, while those greater than - 40 kJ mol^{-1} are corresponding to chemisorptions. The calculated values of ΔG^0_{ads} obtained in this study range between -30.50 kJ mol^{-1} and - 31.82 kJ mol^{-1}, indicating both physical and chemical adsorption behaviour of CPOM on the metal surface. These values indicate that the adsorption process may involve complex interactions involving both physical and chemical adsorption of the inhibitor [33]. The fact that both ΔG^0_{ads} and inhibition efficiency decrease with the increase in temperature, indicates that the adsorption of CPOM on the weld aged maraging steel surface in 2.0 M HCl are not favoured at high temperature and hence can be considered to be predominantly physisorption. The ΔS^0_{ads} value is large and negative; indicating that decrease in disordering takes place on going from the reactant to the alloy adsorbed species. This can be attributed to the fact that adsorption is always accompanied by decrease in entropy [30].

Mechanism of corrosion inhibition: The mechanism of inhibition and the effect of inhibitor in aggressive acidic environment on the metal require some knowledge of interaction between the protective compound and the metal surface. The adsorption mechanism for a given inhibitor depends on factors, such as the

nature of the metal, the corrosive medium, the pH, and the concentration of the inhibitor as well as the functional groups present in its molecule, since different groups are adsorbed to different extents [13]. Inhibitive action of CPOM on the corrosion of weld aged maraging steel in acidic solutions can be explained on the basis of adsorption. The adsorption of CPOM molecules on the metal surface can be attributed to the presence of electronegative elements like oxygen and also to the presence of π electron cloud in the benzene ring of the molecule. CPOM inhibits the corrosion by controlling both the anodic and cathodic reactions.

In HCl solution, the following mechanism is proposed for the corrosion of iron and steel. There are two reactions occur the anodic reaction and cathodic reaction. According to this mechanism anodic dissolution of iron takes place as follows: [30]

$$Fe + Cl^{-} \rightleftharpoons (FeCl^{-})_{ads} \quad (16)$$

$$(FeCl^{-})_{ads} \rightleftharpoons (FeCl)_{ads} + e^{-} \quad (17)$$

$$(FeCl)_{ads} \rightarrow (FeCl^{+})_{ads} + e^{-} \quad (18)$$

$$(FeCl^{+})_{ads} \rightleftharpoons Fe^{+2} + Cl^{-} \quad (19)$$

The nickel present in the maraging steel also undergoes anodic dissolution as follows: [48]

$$Ni + Cl^{-} \rightarrow (NiCl^{-})_{ads} \quad (20)$$

$$(NiCl^{-})_{ads} \rightarrow (NiCl)_{ads} + e^{-} \quad (21)$$

$$(NiCl)_{ads} \rightarrow (NiCl^{+}) + e^{-} \quad (22)$$

$$(NiCl^{+}) \rightarrow Ni^{+} + Cl^{-} \quad (23)$$

The cathodic reaction, hydrogen evolution takes place as follows: [30]

$$Fe + H^{+} \rightleftharpoons (FeH^{+})_{ads} \quad (24)$$

$$(FeH^{+})_{ads} + e^{-} \rightleftharpoons (FeH)_{ads} \quad (25)$$

$$(FeH)_{ads} + H^{+} + e^{-} \rightarrow Fe + H_2 \quad (26)$$

Following mechanisms can be proposed for HER on electrodes in acidic media [20].

a) primary discharge step (Volmer reaction)

$$M + H_3O^{+} + e \leftrightarrow MH_{ad} + H_2O \quad (27)$$

b) an electrochemical-desorption step (Heyrowsky reaction)

$$MH_{ad} + H_3O^{+} + e \rightarrow M + H_2 + H_2O \quad (28)$$

c) a recombination step (Tafel reaction)

$$MH_{ad} + MH_{ad} \rightarrow 2M + H_2 \quad (29)$$

d) For hydrogen evolution reaction, the cathodic reaction may have three different steps: Firstly, hydronium ion is discharged on electrode surface to produce hydrogen atom in acidic solution then three states for the formulation of the mechanism occurs, no one of the three reactions formulated occurs as a single step but combines with another; i.e. Volmer reaction (slow) with the following Heyrowsky (faster) or Tafel (faster) reaction must be. If Volmer reaction is fast, Tafel and/or Heyrowsky reaction must be slow. The step of a slow reaction follows by a fast step. So, presence of inhibitors may hinder the formation of MH_{ad} and suppress reaction or hinder the electron transfer to H_3O^+ ion and suppress reaction [46]. In a corrosive environment, the majority of the adsorbed atomic hydrogen (MH_{ads}) will recombine and form molecular hydrogen, which accumulates and bubbles off of the surface. This recombination of the adsorbed hydrogen atoms is the second step of the HER. This step can take place through an atom-atom combination as suggested by the chemical recombination mechanism (Tafel-Volmer) or through an ion-atom reaction as suggested by the electrochemical recombination mechanism (Volmer - Heyrovsky) [19-20].

It is considered that in acidic solution the CPOM molecule can undergo protonation at its methoxy group and can exist as a protonated positive species. The protonated species gets adsorbed on the cathodic sites of the metal surface through electrostatic interaction, thereby decreasing the rate of the cathodic reaction [49]. In a highly acidic medium like the one in the present investigation, the metal surface is positively charged. This would cause the negatively charged chloride ions to become adsorbed on the metal surface, making the metal surface negatively charged. The positively charged protonated CPOM molecules can interact electrostatically with the negatively charged chloride adsorbed metal surface, resulting in physisorption. The negative charge centres of the CPOM molecules containing a lone pair of electrons and/or π electrons can electrostatically interact with the anodic sites on the metal surface and get adsorbed. The neutral inhibitor molecules may occupy the vacant adsorption sites on the metal surface through the chemisorption mode involving the displacement of water molecules from the metal surface and sharing of electrons by the hetero atoms like oxygen, chloride or bromine with iron. Chemisorption is also possible by the donor -acceptor interactions between π electrons of the aromatic ring and the vacant d orbitals of iron, providing another mode of protection.[50-51] The presence of CPOM in the protonated form and the presence of negative charge centres on the molecule are also responsible for the mutual interaction of inhibitor molecules on the alloy surface [52-56]. This is reflected in the deviation of slopes of Langmuir adsorption isotherms as discussed in the previous section.

SEM / EDS Studies: In order to differentiate between the surface morphology and to identify the composition of the species formed on the metal surface after its immersion in 2.0 M HCl in absence and presence of CPOM, SEM/EDS investigations were carried out. Fig. 9 (a) represents SEM image of corroded weld aged maraging steel sample. Figure 9 (a) shows the facets due to the attack of hydrochloric acid on the metal surface with cracks and rough surfaces. The attack by HCl is seen to be more at grain boundary since these regions are highly susceptible to corrosion. Fig. 9 (b) represents SEM image of weld aged maraging steel after the corrosion tests in a medium of sulphuric acid containing 1.0 mM of CPOM. The image clearly shows the adsorbed layer of inhibitor molecules on the alloy surface thus protecting the metal from corrosion.

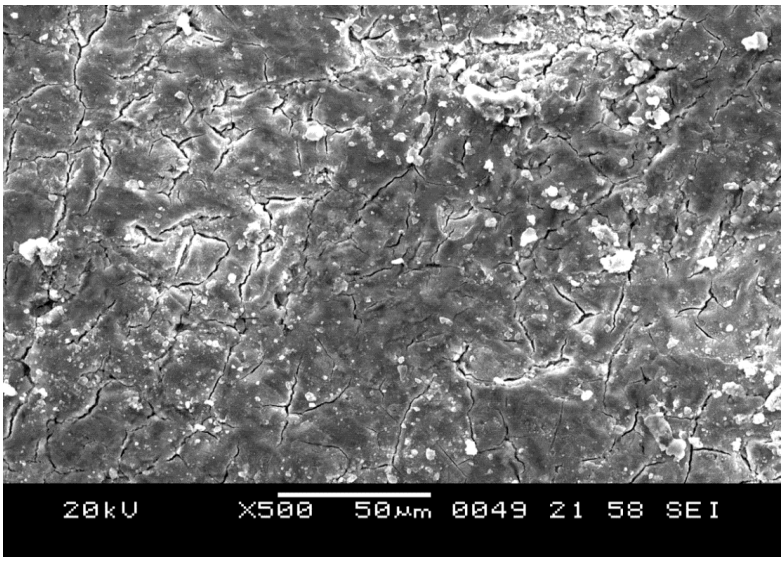

Fig. 9 (a)

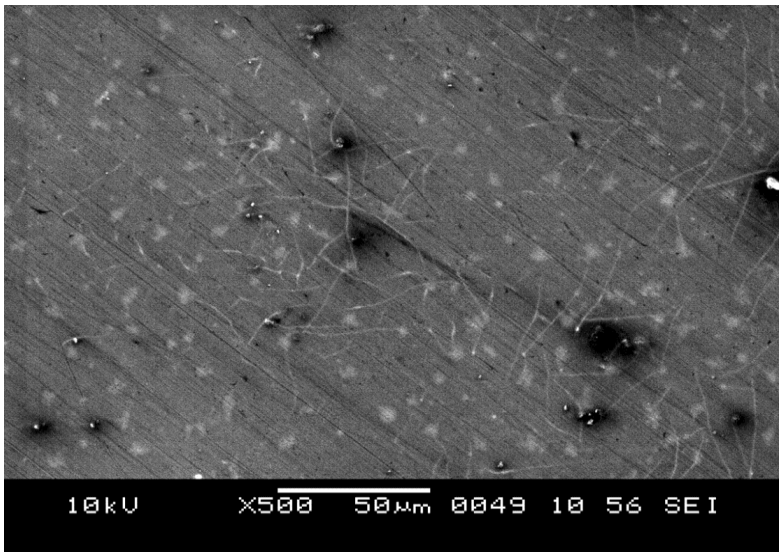

Fig. 9 (b)

Fig. 9 SEM images of the weld aged maraging steel after immersion in 2.0 M HCl a) in the absence and b) in the presence of CPOM.

Therefore, it can be concluded that the smooth and much less corroded morphology of specimens might be attributed to the adsorption of CPOM on the metal surface to suppress the corrosion. EDS investigations were carried out in order to identify the composition of the species formed on the metal surface after its immersion in 2.0 M HCl in absence and presence of CPOM. The corresponding EDS profile analyses for the selected areas on the SEM images 9 (a) and 9 (b) are shown in Fig. 10 (a) and Fig. 10 (b), respectively. The atomic percentage of the elements found in the EDS profile for corroded metal surface were 12.29 % Fe, 3.47 Ni, 4.32% Mo, 73.65% O, 1.75 % Co and 6.57% S and indicated that iron oxide is existing in this area. These elemental composition prove that the corrosion of weld aged maraging steel through the formation of oxide layer. The atomic percentage of the elements found in the EDS profile for less corroded metal surface were 5.20 % Fe, 0.62% Ni, 1.20% Mo, 15.19% O, 2.66% Cl, 70.56% C and 4.37% Br and indicated that formation of inhibitor film in this area. The elemental composition mentioned above was mean value of different regions.

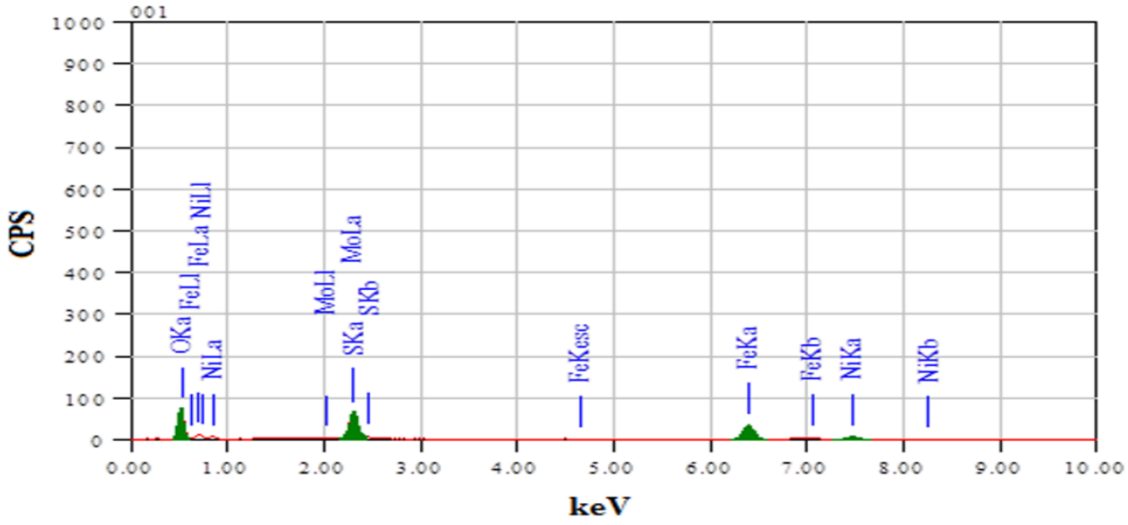

Fig. 10 (a)

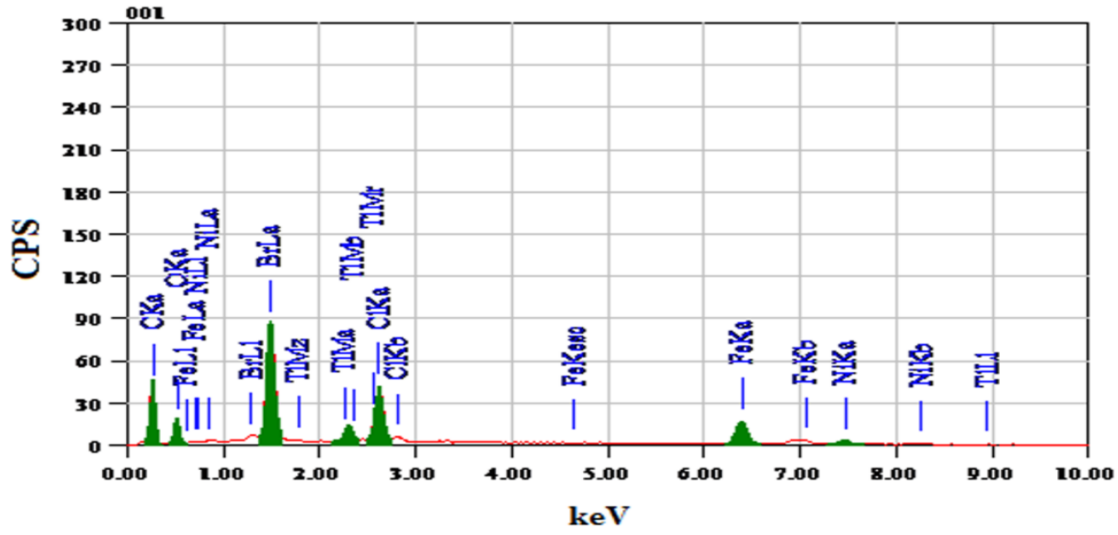

Fig. 10 (b)

Fig. 10 EDS analysis of the weld aged maraging steel after immersion in 2.0 M HCl a) in the absence and b) in the presence of CPOM

APPLICATIONS

Maraging steels are used in the manufacture of engine components like crankshafts, gears, bicycle frames, fencing blades, surgical components and many more. So due to variety of applications they are exposed to different environmental conditions. A study on corrosion inhibition of weld aged maraging steel in acid media gives the detailed information on inhibition mechanism, adsorption behaviour along with the stability of the inhibitor at different concentrations and different temperatures. The calculated thermodynamic parameters confirm the effectiveness of the inhibitor CPOM in acid media.

CONCLUSIONS

The following conclusions may be drawn from the study:

1) 2-(4-bromophenyl)-2-oxoethyl 4-chlorobenzoate (CPOM) acts as an inhibitor for the corrosion of weld aged maraging steel in 2.0 M HCl by affecting both anodic dissolution and hydrogen evolution reactions.
2) The polarisation results showed that corrosion current density (i_{corr}) value or hydrogen evolution rate increases with either increasing temperature or decreasing inhibitor concentration.
3) The EIS results showed that Charge transfer (R_{ct}) and film resistance (R_f) value increases with increasing inhibitor concentration suggesting hindrance for hydrogen evolution and metal dissolution, suggesting decrease in corrosion rate.
4) The adsorption of CPOM was found to follow the Langmuir's adsorption isotherm. The calculated activation and thermodynamic parameters were indicating that the inhibition process occurs via physical adsorption.
5) The SEM/EDX observation proves that the inhibition of corrosion is due to formation of an adsorbed passive film on the metal surface.

REFERENCES

[1] Y.J. Lee, M.C. Kung, Lee, K. I.; Chou, C.P. Effect of lath microstructure on the mechanical properties of flow-formed C-250 maraging steels, *Mater. Sci. Eng. A,* **2007**, 454 – 455, 602- 607.
[2] K. Stiller, F. Danoix, A. Bostel, Investigation of precipitation in a new maraging stainless steel, *Appl. Surf. Sci*, **1996**, 94, 326.
[3] C. Menapace, I. Lonardelli, A. Molinari, Phase transformation in a nanostructured M300 maraging steel obtained by SPS of mechanically alloyed powders, *J. Therm. Anal. Calorim*, **2010**, 101, 815.
[4] M. Nageswara Rao, M. K. Mohan, P. Uma Maheswara Reddy, Environmentally assisted cracking of 18%Ni maraging steel, *Corros. Sci,* **2009**, 51, 1645 - 1650.
[5] W. Wang, W. Yan, Q. Duan, Y. Shan, Z. Zhang, K. Yang, Study on fatigue property of a new 2.8 GPa grade maraging steel, *Mater. Sci. Eng. A*, **2010**, 527, 3057- 3063.
[6] S.Hossein Nedjad, J. Teimouri, A.Tahmasebifar, H. Shirazib, M. Nili Ahmadabadi, A new concept in further alloying of Fe-Ni-Mn maraging steels, *Scr. Mater*, **2009**, 60, 528–531.
[7] T.Poornima, J. Nayak, A.N. Shetty, Studies on corrosion of annealed and aged 18 ni 250 grade maraging steel in sulphuric acid medium, *Port. Electrochim. Acta*, **2010**, 28(3), 173-188.
[8] W.W. Krick, R.A.Covert, T.P. May, Corrosion behavior of high strength steels in marine environment, *Met Eng Quart.*, **1968,** 8, 31.
[9] G.Bellanger, Effect of carbonate in slightly alkaline medium on the corrosion of maraging steel, *J. Nucl. Mater*, **1994**, 217, 187.
[10] G.Bellanger, J.J. Rameau, Effect of slightly acid pH with or without chloride in radioactive water on the corrosion of maraging steel, *J. Nucl. Mater*, **1996,** 228, 24.
[11] J. Rezek, I.E. Klein, J. Yhalom, Structure and Corrosion Resistance of Oxides Grown on Maraging Steel in Steam at Elevated Temperatures, *Appl. Surf. Sci*, **1997**, 108, 159 - 165.
[12] T.Poornima, J. Nayak, A.N. Shetty, Corrosion of aged and annealed 18 Ni 250 grade maraging steel in phosphoric acid medium, *Int. J. Electrochem. Sci*, **2010**, 5, 56 –71.
[13] T. Poornima, J. Nayak, A.N. Shetty, 3, 4 - Dimethoxy benzaldehyde thiosemicarbazone as corrosion inhibitor for aged 18Ni 250 grade maraging steel in 0.5 M sulfuric acid, *J. Appl. Electro chem.*, **2011**, 41, 223 - 233.
[14] T. Poornima, J. Nayak, A.N. Shetty, Effect of 4-(N,N-diethylamino)benzaldehyde thiosemi carbazone on the corrosion of aged 18 Ni 250 grade maraging steel in phosphoric acid solution, *Corros. Sci,* **2011**, 53, 3688 - 3696.

[15] B.S. Sanatkumar, J. Nayak, A.N. Shetty, The corrosion inhibition of maraging steel under weld aged condition by 1(2E)-1-(4-aminophenyl)-3-(2-thienyl)prop-2-en- 1-one in 1.5 M hydrochloric acid medium, *J. Coat. Technol. Res,* DOI 10.1007/s11998-011-9379-1.
[16] Y.Yan, W. Li, L. Cai, B. Hou, Electrochemical and quantum chemical study of purines as corrosion inhibitors for mild steel in 1M HCl solution, *Electrochim. Acta*, **2008**, 53, 5953–5960.
[17] R. Solmaz, G. Kardaş, M. Culha, B. Yazıcı, M. Erbil, Investigation of adsorption and inhibitive effect of 2-mercaptothiazoline on corrosion of mild steel in hydrochloric acid media, *Electrochim. Acta*, **2008**, 53, 5941–5952.
[18] K.F.Khaled, N. Hackerman, Investigation of the inhibitive effect of ortho-substituted anilines on corrosion of iron in 1 M HCl solutions, *Electrochim. Acta,* **2003**, 48, 2715- 2723.
[19] N.F.Atta, A.M. Fekry, H.M. Hassaneen, Corrosion inhibition, hydrogen evolution and antibacterial properties of newly synthesized organic inhibitors on 316L stainless steel alloy in acid medium, *Int. J. Hydrogen Energy*, **2011**, 36, 6462-6471.
[20] A.M. Fekry, M.A. Ameer, Corrosion inhibition of mild steel in acidic media using newly synthesized heterocyclic organic molecules, *Int. J. Hydrogen Energy,* **2010**, 35, 7641 - 7651.
[21] S.S. Abd EL-Rehim, M.A.M. Ibrahim, K.F. Khaled, 4-Aminoantipyrine as an inhibitor of mild steel corrosion in HCl solution, *J. Appl. Electrochem*, **1999**, 29, 593-599.
[22] G.Y. Elewady, Pyrimidine derivatives as corrosion inhibitors for carbon-steel in 2m hydrochloric acid solution, *Int. J. Electrochem. Sci*, **2008**, 3, 1149 - 1161.
[23] H.K. Fun, C.S. Yeap, B. Garudachari, A.M. Isloor, M.N. Satyanarayan, 2-(4-Bromophenyl)-2-oxoethyl 4-chlorobenzoate, *Acta Crystallogr., Sect. E:* **2011**, E67, 1723.
[24] L.T. Kelly, H.W. Howard, Phenacyl and p-bromophenacyl esters of monosubstituted benzoic acids, *J. Am. Chem. Soc,* **1932**, 54, 4383-4385.
[25] S.W. Dean, Standard practice for calculation of corrosion rates and related information from electrochemical measurements, Norm ASTM G102, **1999**, 2-3.
[26] R.A. Prabhu, T.V. Venkatesha, A.V. Shanbhag, G.M. Kulkarni, R.G. Kalkhambkar, Inhibition effects of some Schiff's bases on the corrosion of mild steel in hydrochloric acid solution, *Corros. Sci*, **2008**, 50, 3356 -3362.
[27] Z. Tao, S. Zhang, W. Li, B. Hou, Adsorption and inhibitory mechanism of 1H-1,2,4-Triazol-l-yl-methyl- 2-(4-chlorophenoxy) acetate on corrosion of mild steel in acidic solution, *Ind. Eng. Chem. Res*, **2011**, 50, 6082 - 6088.
[28] Z. Tao, S. Zhang, W. Li, B. Hou, Adsorption and corrosion inhibition behavior of mild steel by one derivative of benzoic-triazole in acidic solution, *Ind. Eng. Chem. Res*, **2010**, 49, 2593–2599.
[29] W. Li, Q. He, C. Pei, B. Hou, Experimental and theoretical investigation of the adsorption behaviour of new triazole derivatives as inhibitors for mild steel corrosion in acid media, *Electrochim. Acta*, **2007**, 52, 6386-6394.
[30] S. Ashish Kumar, M.A. Quraishi, Effect of cefazolin on the corrosion of mild steel in hcl solution, *Corros. Sci*, **2010**, 52, 152–160.
[31] W.H. Li, Q. He, S.T. Zhang, C.I. Pei, B.R. Hou, Some new triazole derivatives as inhibitors for mild steel corrosion in acidic medium, *J. Appl. Electrochem*, **2008**, 38, 289 - 295.
[32] A.S. Fouda, F.E. Heakal, M.S. Radwan, Role of some thiadiazole derivatives as inhibitors for the corrosion of c-steel in 1 m h2so4, *J. Appl. Electrochem*, **2009**, 39, 391- 402.
[33] E. Machnikova, H. Kenton Whitmire, N. Hackerman, Corrosion inhibition of carbon steel in hydrochloric acid by furan derivatives, *Electrochim. Acta*, **2008**, 53, 6024-6032.
[34] A.Yagan, N.O. Pekmez, A. Yıldız, Electrochemical synthesis of poly (N-methylaniline) on an iron electrode and its corrosion performance, *Electrochim. Acta,* **2008**, 53, 5242-5251.
[35] I. Dehri, M. Erbil, The effect of relative humidity on the atmospheric corrosion of defective organic coating materials: an EIS study with a new approach, *Corros. Sci,* **2000**, 42, 969-978.
[36] X. Wang, H. Yang, F. Wang, A cationic gemini-surfactant as effective inhibitor for mild steel in HCl solutions, *Corros. Sci*, **2010**, 52, 1268-1276.

[37] A. EL-Sayed, Phenothiazine as inhibitor of the corrosion of cadmium in acidic solutions, *J. Appl. Electrochem,* **1997**, 27,193-200.
[38] S.T. Arab, Inhibition action of thiosemicabazone and some of it is α-substituted compounds on the corrosion of iron-base metallic glass alloy in 0.5 M H2SO4 at 30 ˚C, *Mater. Res. Bull,* **2008**, 43, 510 - 521.
[39] M. Ozcan, I. Dehri, M. Erbil, Organic sulphur-containing compounds as corrosion inhibitors for mild steel in acidic media: correlation between inhibition efficiency and chemical structure, *Appl. Surf. Sci*, **2004**, 236, 155–164.
[40] M.P. Geetha, J. Nayak, A.N. Shetty, Corrosion inhibition of 6061Al-15vol.pct.SiC(p) composite and its base alloy in a mixture of sulphuric acid and hydrochloric acid by 4-(N,N-dimethylamino) benzaldehyde thiosemicarbazone, *Mater. Chem. Phys*, **2011**, 125, 628-640.
[41] M. Bouklah, B. Hammouti, A. Aounti, T. Benhadda, "Thiophene derivatives as effective inhibitors for the corrosion of steel in 0.5 M H2SO4, *Prog Org Coat*, **2004**, 49 227.
[42] G. Avci, Corrosion inhibition of indole-3-acetic acid on mild steel in 0.5M HCl, *Colloids Surf. A,* **2008**, 317, 730 -736.
[43] M. Sahin, S. Bilgic, H. Yilmaz, The inhibition effects of some cyclic nitrogen compounds on the corrosion of the steel in NaCl mediums, *Appl. Surf. Sci*, **2002**, 195, 1-7.
[44] B. Ateya, B.E. El-Anadouli, F.M. El-Nizamy, The adsorption of thiourea on mild steel, *Corros. Sci*, **1984**, 24, 509 -515.
[45] E.E. Oguzie, V.O. Njoku, C.K. Enenebeaku, C.O. Akalezi, C. Obi, Effect of hexamethyl pararosaniline chloride (crystal violet) on mild steel corrosion in acidic media, *Corros. Sci*, **2008**, 50, 3480 - 3486.
[46] A.M. Fekry, M.A. Ameer, Electrochemical investigation on the corrosion and hydrogen evolution rate of mild steel in sulphuric acid solution, *Int. J. Hydrogen Energy*, **2011**, 36, 11207 -11215.
[47] R.A. Prabhu, A.V. Shanbhag, T.V. Venkatesha, Influence of tramadol [2-[(dimethylamino) methyl]-1-(3- methoxyphenyl) cyclohexanol hydrate] on corrosion inhibition of mild steel in acidic media, *J Appl Electrochem*, **2007**, 37, 491- 497.
[48] G.Burstein, G. Wright, The anodic dissolution of nickel- ii. Bromide and iodide electrolytes, *Electrochim. Acta*, **1976**, 21, 311- 314.
[49] N. Hackerman, E.S. Snavely, J.S. Jr. Payne, ''Effects of anions on corrosion inhibition by organic compounds,'' *J. Electrochem. Soc*, **1966**, 113 677–686.
[50] A.K. Satpati, P.V. Ravindran, Electrochemical study of the inhibition of corrosion of stainless steel by 1,2,3-benzotriazole in acidic media, *Mater. Chem. Phys*, **2008**, 109 352–359.
[51] E. Blomgren, J.O.M. Bckris, The adsorption of aromatic amines at the interface: mercury-aqueous acid solution, *J. Phys. Chem*, **1959**, 63, 1475.
[52] A.S. Fouda, G.Y. Elawady, W.T. Elbehairy, Adsorption and Protection of Low C-Steel Corrosion in 1M Hydrochloric acid Medium using Hyoscyamus Muticus Plant Extract, *J Applicable Chem.*, **2017**, 6 (1), 69-83.
[53] S.K. Rajappa, T.V. Venkatesh, Corrosion Protection Studies of Modified Mild Steel Surface in Hydrochloric Acid Medium, *J Applicable Chem.*, **2015**, 4 (1), 212-220.
[54] Alpana Soni, Pratibha Sharma, Monika, Rekha Dashora and A.K.Goswami, Corrosion Inhibition of Brass in 0.5N HNO_3 By 3-Hydroxy-3-(4-Chlorophenyl- 1-(4-Sulphonato (Sodium Salt)) Phenyl Triazene (HCST): Adsorption and Thermodynamic Study, *J. Applicable. Chem*., **2016**, 5 (1): 281-290.
[55] Nil Desai S, Malik G.M, Inhibition Study of Caesalpinia Crista on Corrosion of Mild Steel in Sulphuric acid, *J.Applicable.Chem.*, **2016**, 5 (5): 1226-1235.
[56] Doddahosuru M. Gurudatt and Kikkeri N. Mohana. Synthesis of New Benzimidazole Derivatives And Their Corrosion Inhibition Performance On Mild Steel In 0.5 M Hydrochloric Acid, *J. Applicable. Chem*., **2013**, 2 (5):1296-131.

AUTHORS' ADDRESSES

1. **Dr. Sanatkumar B.S.**
Assistant Professor in Chemistry, Department of Basic Science and Humanities
Agnel Institute of Technology and Design, Assagao, Bardez, Goa - 403 507, India
sanatkumarbs@gmail.com, Phone: +919970558477

2. **Dr. A. Nityananda Shetty**
Professor in Chemistry,
National Institute of Technology of Karnataka. Surathkal - 575 025, Karnataka, India
nityashreya@gmail.com, Mob: +919448779922